ALEPH 90-29
PHYSIC 90-13
S. Brandt et al.
28.2.1990

Systematic studies on the Luminosity

SIEGEN group, S.Brandt, H.Burkhardt, C.Grupen, H.Meinhard,
E.Neugebauer, H.Seywerd

27 February 1990

1 Introduction

An Aleph Note with details on luminosity errors for the first Aleph publication [1] has been made available recently [2]. The second Aleph publication on the line shape [3] quotes now 1.3 % error on absolute luminosity (1.05 % experimental based on the LCAL alone and 0.7 % theoretical). This is an excellent result and substantially smaller than the precision reached in previous e^+e^- experiments. In this note we describe a number of additional studies and independent checks.

2 Standard cuts

The standard analysis used in both line shape publications is based on the so called method five cuts. The energy cuts and the fiducial cuts were tightened for the second publication [3]. The algorithm of method five looks for the most energetic cluster on each LCAL side and requires:

- $E_{clus}/E_{beam} > 20\ GeV/45.5\ GeV$ for each side
- sum of $E_{clus}/(2E_{beam}) > 0.6$
- $\Delta\phi > 170$ degrees (or acoplanarity less than 10 degrees)
- small fiducial cut on side A (B) for even (odd) event number
- large fiducial cut on side B (A) for odd (even) event number

Only information from the most energetic cluster on each side is used. This has implications for extra photons from higher order Bhabha diagrams. The size of a cluster is limited to the physical boundaries of the calorimeter and to towers with energies above threshold. Two showers in the same LCAL module within a distance of about 15 cm are generally reconstructed as though they were a single cluster.

The details of the present fiducial cuts are rather complicated and very much connected with the internal geometry of the LCAL, but important for a precise discussion of the

uncertainty in the luminosity determination. In doing comparisons with the SATR and carefully checking the LCAL code we found that the implementation of the fiducial cuts is in fact not quite as originally intended and as described in the line shape publication.

2.1 Fiducial Region Cuts

The LCAL is read out longitudinally in 3 stories and the tower with the highest energy is generally in the second storey representing 10.4 radiation lengths. On the edges of the calorimeter the pads used in constructing the towers have a smaller size than those further inside. Such towers are excluded from the fiducial region on the inside edge. Along the outside edge the cut approximates an angular cut of 110 mrad, following the edges of tower boundaries. This is in order to avoid regions shadowed by dead material (e.g. the TPC support), which are poorly simulated by Monte Carlo and give rise to discrepancies in the tails of energy loss distributions in comparison between the GALEPH Monte-Carlo and data.

The large fiducial cut uses position information determined from the reconstructed cluster position. It requires the distance between the reconstructed shower centroid and the inner LCAL boundary to be greater than 1.0 cm in Δx and 0.75 cm in Δy and the reconstructed θ to be less than 125 mrad.

The algorithm for determining if an event is in the small fiducial cut region proceeds as follows:

- The same cut as that applied to the large fiducial region side is first made on the small fiducial region side as well. Here however it has almost no effect. If we would leave this cut out, we gain very few events (order 10^{-4}) by the 1.0 cm Δx cut and no events by the Δy cut.

- If the tower containing the highest energy is outside the set of allowed towers, the event is rejected. We found that this cut almost entirely limits the acceptance. Only a very small fraction of events is rejected by further cuts.

- For events along the inner horizontal boundaries, another cut is applied: The energy sum of triplets of towers, using only the energy in the first LCAL storey (4.7 radiation lengths), is compared. Since the lateral shower width is rather small, a lot of energy is generally contained in the central tower and the transition between the energy in one tower row and the next is very sharp. In other words, the position resolution of the LCAL is best on the border between towers. A way to look at this is to plot energy asymmetries (E_{in}-E_{out} normalized to their sum) as discussed in [2]. The triplet within the fiducial volume is required to have more energy than the one just outside the boundary, i.e. the asymmetry from (E_{in}-E_{out}) must be positive ("asymmetry cut"). We found that this in fact was done along the horizontal boundary, only for showers with $y > 0$. For showers with $y < 0$, the comparison was done incorrectly, using a triplet further inside the fiducial volume.

- The analogous asymmetry cut at the vertical boundary was only applied (incorrectly) along columns two and ten which are the very inside and outside vertical limits. There

was, though, no cut made for the large fraction of events with the highest tower in row five, which is the vertical boundary close to the horizontal plane.

- Numerically we found that 18 % (1887 out of 10593) of the events are tested on the asymmetry cut. Since the highest tower has already been required to be within the allowed range, only $1.6 \cdot 10^{-3}$ in data (and $1.48 \cdot 10^{-3}$ in Monte Carlo) of events are rejected by the energy asymmetry cut. Due to the dominance of the cut on the highest tower and the incorrect implementation of the energy-asymmetry cut the systematic check mentioned in [3] exchanging the first and second storey in the asymmetry calculation is of little relevance.

To our knowledge these are the cuts that have been applied in the standard method five as used for the second line shape paper [3]. In the meantime the errors and inconsistencies, discussed above, have been corrected in the more recent versions of the luminosity calculation programs. Since method five has always been consistently applied to both data and Monte Carlo the resulting luminosity is essentially equal as determined with the old and the new program version.

	MT - Stor1 method 5	Stor2 - Stor1 method 5	MT - Stor1 method 6	Stor2 - Stor1 method 6
data	0.15 %	0.12 %	0.33 %	0.38 %
MC	0.27 %	0.42 %	0.23 %	0.44 %
diff	0.12 %	0.30 %	0.10 %	0.06 %

Table 1: Comparison of fiducial cuts based on the maximum tower (MT) or energy asymmetries using only the first or second storey of the LCAL (numbers from F.Bird, based on about 20 000 data and 45 000 Monte Carlo events)

Table 1 compares three different ways to define the acceptance. MT stands for maximum tower or the selection that has been described here. Stor1 and Stor2 denote the selection based on energy asymmetries using only the first or second storey of the LCAL. Using energy asymmetries based on storey one (as originally intended) instead of the central tower to define the acceptance for example would reduce the accepted sample by 0.15 %. The Monte Carlo predicts 0.27 % and the luminosity would change therefore by 0.12 %. This is well within the range of the systematic error. The main conclusions in this note do not depend on the details of the definition of the fiducial cut. In general we will continue the discussion with the selection as used in the second line shape paper.

2.2 Energy Cut

The effect of the energy cut is illustrated in figure 1 for various data samples. Sample a) consists of all events with any LCAL trigger bit set. Sample b) requires the coincidence bits and the position of both clusters to be within the tight fiducial region of the so called method six. Method six makes a further acceptance cut with respect to that of method five by requiring that clusters have a distance to the edge of the sensitive area of the

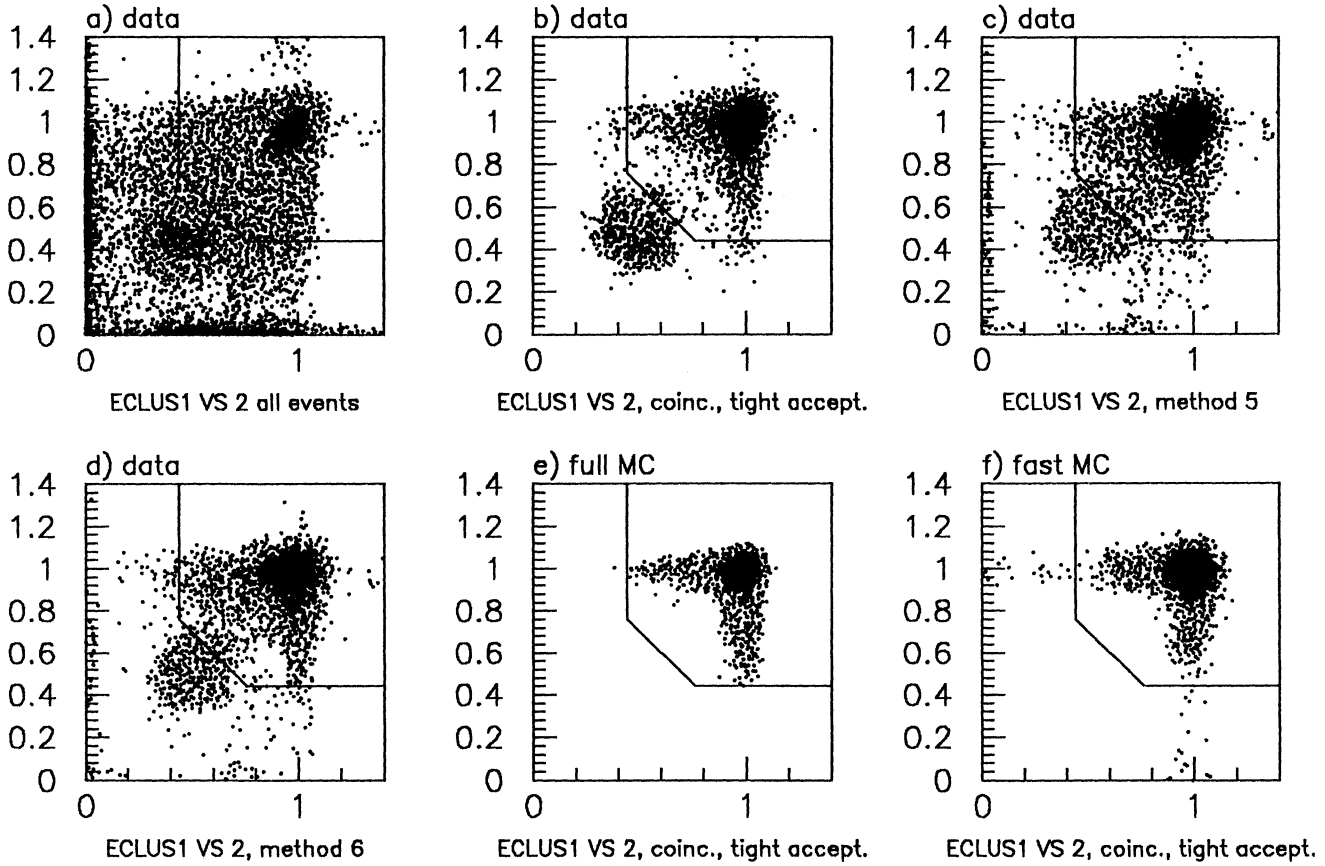

Figure 1: Eclus1 versus Eclus2 for various data and Monte Carlo samples. The energies are normalized to the beam energy.

calorimeter of at least one full pad size. For this plot the tight fiducial cut has been applied on both sides, to better illustrate the separation of background and data. No other cuts, and in particular no cuts on energy or on $\Delta\phi$ have been applied. One can see, that the data peaks with both cluster energies at the beam energy. The off momentum particle background clusters close to 50 % of the beam energy. On the low side all clusters are rejected by the trigger thresholds (between 16 and 20 GeV or 0.35 - 0.44 of the beam energy for the coincidence trigger). Note that the requirement of having both clusters well inside the LCAL alone very cleanly separates Bhabhas and background. The plots c), d) are from event data samples after having applied the cuts of method five and six except for the energy cut. Eclus1 is the energy from the side with the small and Eclus2 the energy from the side with the large fiducial cut. One can see that the background peak is reduced through the $\Delta\phi$ cut. The separation between Bhabhas and background for Eclus2 is less clean since events near the edge with energy leakage are not rejected by the large fiducial cut. The two plots e), f) are from Monte Carlo data using a first order event generator without any background simulation. Here, the fiducial cuts of method six have been applied on both sides to minimize leakage and to better display the effects of radiative corrections. The statistics are comparable to those of the data event samples.

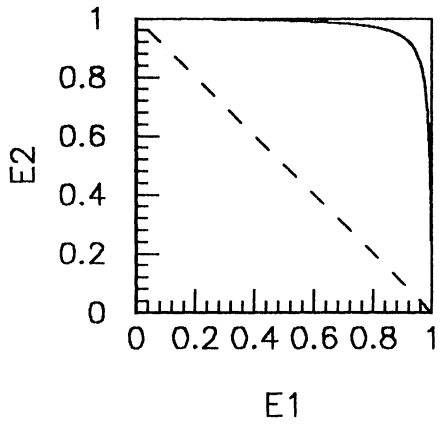

Figure 2: Dalitz plot for 3 body final state. The solid line demonstrates that a tight acollinearity cut of 10 degrees limits the available phase space such, that one of the two clusters has an energy close to that of the beam. The dashed line shows the kinematic limit in absence of cuts.

In the plots of Figure 1 it is also possible to see the typical radiative tails from single gammas. From e^+e^- kinematics for a three body final state of massless particles one gets :

$$E_1 = \frac{2(1 - E_2)}{2 - E_2(1 + cos\zeta)}$$

$E_{1,2}$ are the final state charged particle energies normalized to beam energy and ζ is the acollinearity. Figure 2 illustrates the relation between $E_{1,2}$ for an acollinearity cut of 10 degrees. The limited polar angle acceptance (120 mrad - 50 mrad = 70 mrad $\approx$ 4 degrees) for luminosity implies a still tighter acollinearity condition and therefore that either E_{clus1} or E_{clus2} is practically equal to the beam energy. In absence of shower leakage (as in the

fast Monte Carlo) we expect, therefore, that the maximum of E_{clus1}, E_{clus2} is peaked at the beam energy, without the low energy tail. This feature can be seen in Figure 3. The dotted

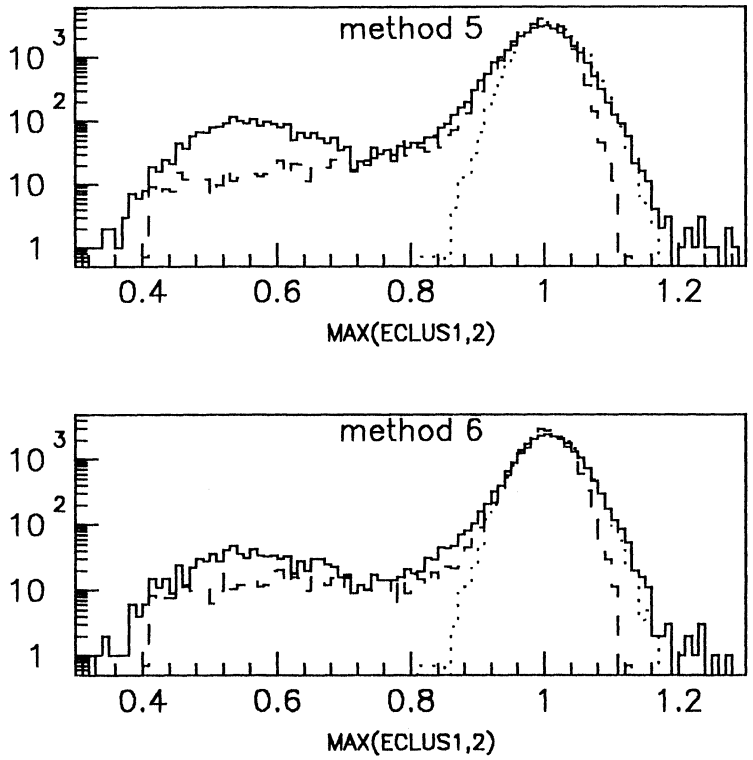

Figure 3: Maximum $Eclus_{1,2}$ for data (solid line), full, and fast Monte Carlo (broken and dotted line). The cuts are method 5,6 without the energy cut. The energies are normalized to the beam energy.

line is from the fast Monte Carlo using a gaussian resolution of 29 % / $\sqrt{E}$. The broken line is the result of the full Monte Carlo which includes shower leakage at the edges. The percentage of events below 0.8 is 0 % for the fast Monte Carlo, 2.1 % for the full Monte Carlo and 6.4 % for the data and illustrates the amount of shower leakage and shower leakage plus background.

To see how the luminosity measurement would change with the energy cut we take the number of events above 0.8 in figure 3 and divide by the number of events accepted using the standard energy cut of method five. We obtain 99.22 % for data, 99.55 % for the full Monte Carlo (100.0 % for the fast Monte Carlo). The difference between data and full Monte Carlo of 99.55 - 99.22 = 0.33 % is consistent with 0.3 % background with standard method five cuts and negligible background in the case of a cut at 0.8 in the maximum of the cluster energies. Table 2 shows the effect of changing the energy cut (numbers by F.Bird). The difference between data and Monte Carlo is $1.5 \cdot 10^{-3}$ or less.

Cut Description	MC (%)	data-bkg (%)	difference (%)
$E_{1,2} > 0.44E_{beam}, E_{SUM} > 1.2E_{beam}$	-	-	0
$E_{1,2} > 0.33E_{beam}, E_{SUM} > 1.2E_{beam}$	+0.09	+0.18	+0.09
$E_{1,2} > 0.55E_{beam}, E_{SUM} > 1.2E_{beam}$	-0.45	-0.54	-0.09
$E_{1,2} > 0.44E_{beam}, E_{SUM} > 1.1E_{beam}$	+0.05	+0.10	+0.05
$E_{1,2} > 0.44E_{beam}, E_{SUM} > 1.3E_{beam}$	-0.07	-0.15	-0.08
$\sqrt{E_1^2 + E_2^2}/E_{beam} > 0.90$	+0.05	+0.16	+0.11
$\sqrt{E_1^2 + E_2^2}/E_{beam} > 0.95$	-0.03	+0.05	+0.08
$\sqrt{E_1^2 + E_2^2}/E_{beam} > 1.00$	-0.16	-0.01	+0.15

Table 2: Variation with energy cut

3 Mini-DST

The POT data for 1989 is rather large and to read it is quite time consuming. The information used for luminosity is only a very small fraction of the full POT data. It is therefore convenient to do the analysis for sets of many runs in two steps. In the first step, all relevant data is written to a special mini-DST. This mini-DST is then used for the analysis in the second step.

The standard method five cuts can be done using the following information:

- Cluster energy
- Maximum tower address
- first storey triplet energy asymmetry in rows and columns ($E_{in} - E_{out}$ normalized to its sum)
- cluster centroid θ and ϕ position
- cluster centroid distance in x, y to the border

This plus some further information is written to the mini DST for every event with any LCAL trigger. The additional information includes reconstructed SATR positions, run and event number, trigger and high voltage status bits. Mini-DSTs, on which all following comparisons are based, have been produced for all data, as well as for the full and fast Monte Carlo.

4 Mini-MC, size of corrections

The full Monte Carlo (GALEPH) has been the basis for the effective cross section calculation. In the first step, the event generator BABAMC [5] is used to produce events in form of four-vectors (e^+, e^-, γ). This is done at the peak assuming $M_Z = 91.0\ GeV$, $m_{top} = m_{higgs} = 100\ GeV$ and for a θ range of 38-200 mrad. As discussed in [9], BABAMC should be used with the modified vacuum polarization routine. Since we use BABAMC

only for small angles we should also follow the recommendation of the event generator group in [6] and run BABAMC with the smallest allowed value of K_0. Using the correct vacuum polarization and K_0=0.001 results in 85.984 $\pm$ 0.008 nb cross section from BABAMC without any cuts. By mistake, an old version of BABAMC was used for the effective cross section in [1], [3] resulting in 86.57 nb cross section at 91.0 GeV which is about 0.6 % too high.

The result of the pure QED program OLDBAB [4] is 85.804 ± 0.015 nb or $(2.36 \pm 0.26) \cdot 10^{-3}$ less than our BABAMC result. The electroweak correction and scaling with energy is described in section 5.

The detector simulation is done using GALEPH and the result is in form of standard raw data files. The JULIA program for reconstruction and selection of events is the same as for real data. For 150 000 events from BABAMC, using the cuts of method five, 46406 have been accepted by JULIA, so that we calculate an effective cross section of $85.984\ nb \cdot 46406/150000 = (26.60 \pm 0.10)\ nb$ at 91.0 GeV.

The computer time involved and the amount of raw data which must be handled does not allow the repetition of the full simulation for various sets of input parameters. We decided instead to write a simple very fast Monte Carlo for that purpose. The sequence KINGAL-event generator, GALEPH, JULIA, Mini-DST production is reduced to a single step. There is no shower simulation. The energy is taken from the event generator and modified assuming gaussian errors only. The position in the LCAL is calculated from the direction of the vectors from the event generator and the true LCAL position, taking into account the magnetic field, geometrical beam parameters, and alignment errors. The calculated position is then converted into a tower address that is used in the cuts of method five. If both clusters are in the same LCAL module and if they are within 15 cm of one another, the electron and photon energies are added and the energy weighted position is calculated. The radiative tails are well reproduced as shown previously in figure 1.

Note that the fast Monte Carlo does not know anything about the internal tower structure of the LCAL nor about shower size. There is no leakage close to the edge. Either the energy is fully inside and added, or completely neglected.

The total cross section, calculated from the fast Monte Carlo, for method five is only 1.1 % less than that calculated from the full Monte Carlo and suggests that the details of the shower development are not very important. The agreement is even better for method six cuts where the fast MC predicts 0.5 % less cross section compared to the full MC.

4.1 Size and uncertainty of radiative corrections

The fast Monte Carlo has also been used together with a lowest order Bhabha generator. In lowest order the e^+e^- are always back to back and have exactly beam energy. The total cross section was found to be $83.808\ nb \cdot 46461/150000 = (25.96 \pm 0.10)\ nb$ at 91 GeV. The first order result of 26.60 nb, is +2.5 % greater. If the first order correction is δ the second order correction is usually assumed to be of order $\delta^2/2$ or $3 \cdot 10^{-4}$ in this case. Since this is a very small number it seems worthwhile to understand if the 2.5 % is a representative number for the first order correction or the result of accidental cancellation of larger numbers. In fact it would have been easy to tune the cuts such that the first order

correction becomes small. We could tighten our cuts (in cluster energy or acoplanarity) and reduce the first order result until it agrees exactly with lowest order.

Asymmetric cuts allow to increase the first order cross section. In lowest order Bhabhas are always back to back and the acceptance is determined by the small side alone. Table 3 shows the percentage of events that are cut if the tight cuts are applied symmetrically on both sides. The reduction is between 7 and 8 % and implies that the first order correction in the symmetric case would be about $\delta = -5\%$.

sample	loss, method 5	loss, method 6
data	$7.8 \pm .2$	$11.0 \pm .2$
full MC	$7.4 \pm .1$	$10.7 \pm .2$
fast MC	$7.0 \pm .1$	$10.8 \pm .2$

Table 3: loss of events in % going from asymmetric to symmetric cuts for data and Monte Carlo and method 5 and 6.

We also checked how many events are lost in the fast Monte Carlo if we do not merge close electrons and photons, but cut on the electron energy alone. The result is that the radiative tails become much more pronounced and that we would loose 1.7 % more events in the energy cut.

To be conservative, we argue that the first order correction is of the order of $\delta = 10\%$ from which we obtain the uncertainty $\delta^2/2 = 0.5\%$ from neglecting of higher orders. Higher order Bhabha programs are presently in preparation[8]. The uncertainty from higher orders is therefore expected to become negligible in the near future. The hadronic uncertainties have been determined using the procedure of reference [9] and are only of order $O(10^{-4})$.

4.2 Physics background contributions

The calculation of the effective accepted cross section has been done using BABAMC limiting the e^+ , e^- at generation to an angular range of 38-200 mrad such that the e^- goes always forward in the Aleph coordinate system. The cuts are such that also events with forward e^+ and backward e^- would be accepted. The cross section from the generators, for an angular range of $\pi - 200mrad$ $\pi - 38mrad$, was found to be about 0.019 nb. Using the fast MC, the effective cross section with method five cuts was found to be 0.004 nb or about $1.5 \cdot 10^{-4}$ of the forward cross section which is completely negligible.

The method five selection does not distinguish between e^+, e^- and γ final states. We tried to estimate the cross section for processes where one or both particles in the final states are photons.

The 1981 version of the Berends/Kleiss Bhabha generator restricts the angular range for the e^+ alone with inclusion of the so called t'-pole events. Using this program, we found an additional contribution from e, γ final states of 0.04 nb or $1.5 \cdot 10^{-3}$ of the forward Bhabha cross section.

We also calculated the effective cross section for e^+, e^- annihilation into photons. L3 adds a 0.5 % contribution from this channel to their luminosity cross section [10]. We

instead believe that this contribution is very small. To check we used both an event generator and analytic calculations. Neglecting masses we obtain in lowest order [11]:

$$\frac{d\sigma}{d\Omega} = \frac{\alpha^2}{2s}\left[\frac{t^2}{u^2} + \frac{u^2}{t^2}\right]$$

Both photons are indistinguishable. To correct for double counting in the integration over the full phase space we include an additional factor $\frac{1}{2}$ in the above formula. Looking now at the ratio e^+e^- annihilation over Bhabha scattering :

$$\frac{d\sigma_{Bhabha}}{d\Omega} = \frac{\alpha^2}{4s}\left[\frac{3+c^2}{1-c}\right]^2 \quad ; \quad \frac{d\sigma_{\gamma\gamma}}{d\Omega} = \frac{\alpha^2}{2s}\left[\frac{1+c^2}{1-c^2}\right]$$

for small angles we have $c = cos\theta \approx 1 - \theta^2/2$ and we get :

$$\frac{d\sigma_{\gamma\gamma}}{d\Omega} / \frac{d\sigma_{Bhabha}}{d\Omega} \approx \frac{\theta^2}{16}$$

At $\theta = 80mrad$ the ratio becomes $4 \cdot 10^{-4}$. From the fast Monte Carlo and using a $\gamma\gamma(\gamma)$ event generator we obtain at W = 91 GeV an effective cross section of 0.012 nb or $4.5 \cdot 10^{-4}$ of the Bhabha cross section.

4.3 Magnetic Field

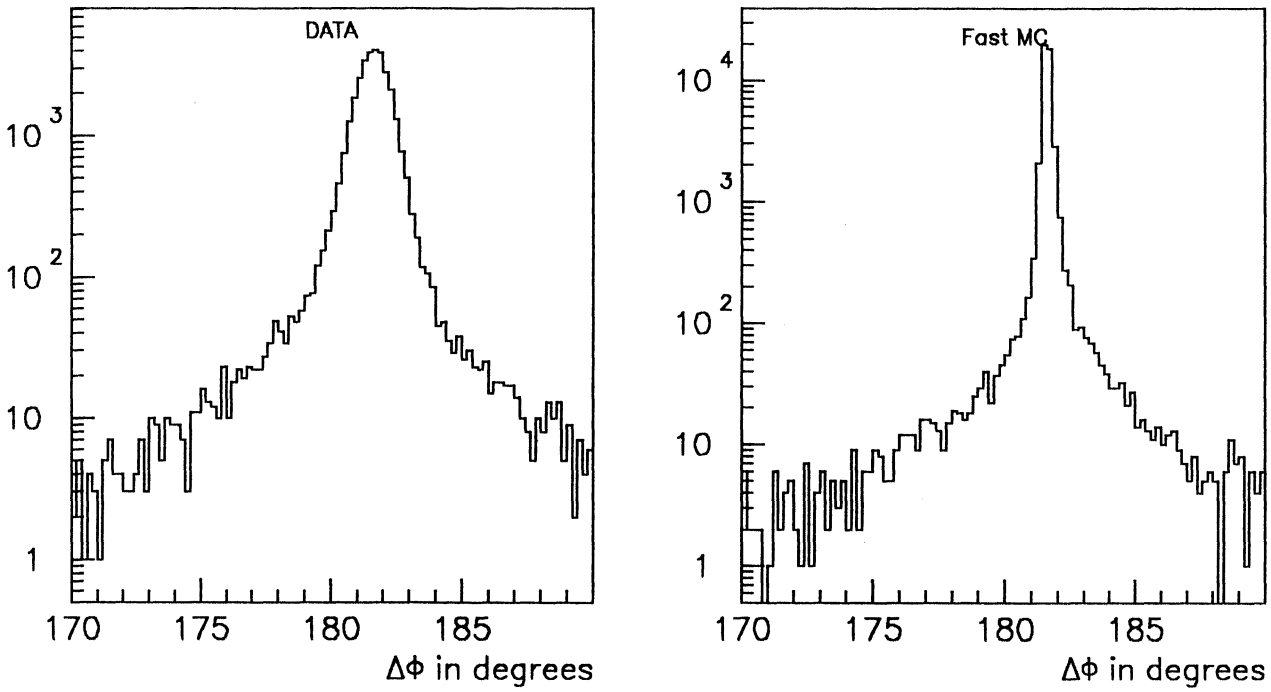

Figure 4: $\Delta\phi$ distribution around 180 degrees

The magnetic field of ALEPH is 1.5 Tesla in electron (+z) direction. The main effect is that the apparent ϕ is modified by

$$\Delta\phi = -\frac{qBz}{2p}$$

i.e. +14 mrad or 0.8 degrees, for an electron with charge q=-e and momentum p=45 GeV/c at the LCAL (z=280 cm). The $\Delta\phi = \phi_1 - \phi_2$ distribution shown in figure 4 does not peak at 180 but rather at 181.6 degrees. The scatter plots in figure 5 illustrate the combined

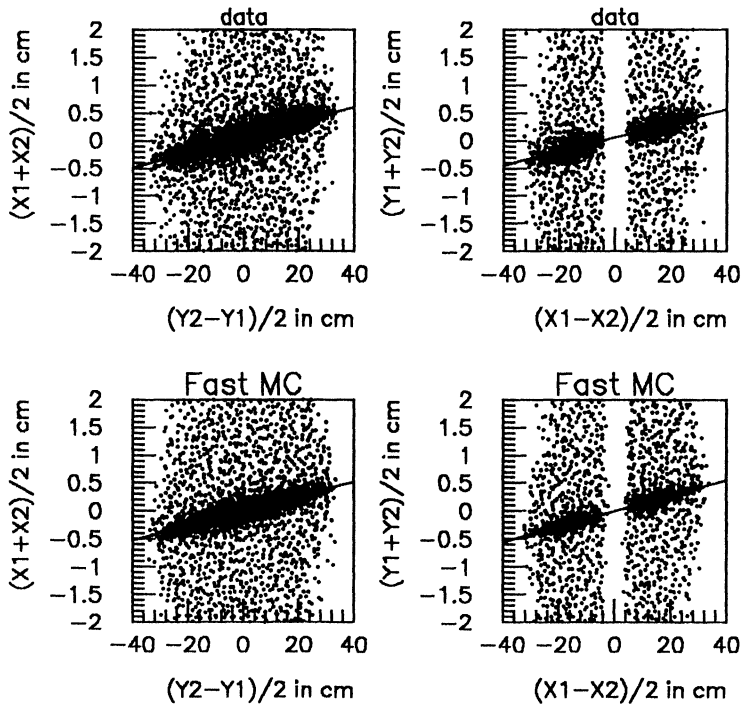

Figure 5: Field effect and straight line fit using the reconstructed x and y positions from the LCAL

effect of the vertex position and the magnetic field (the slope is $\Delta\phi$ and the intercept the vertex position). As can be seen from the figures, the effect of the magnetic field in the data is already well reproduced by the simple Monte Carlo. The vertex position can be determined using a straight line fit and was found to be $x_0 = 0.062$ cm and $y_0 = 0.055$ cm.

4.4 Alignment

The basic assumption in all alignment procedures applied both in Monte Carlo production and in the reconstruction is that the LCAL and the SATR modules (four of which give the complete subdetector) are themselves rigid bodies. Furthermore, we assume that the SATR modules do not have any misalignment as compared to the appropriate LCAL module to which they are mounted. Some feeling about the quality of this assumption, as far as the LCAL is concerned, can be obtained from ref. [2]. From the way the SATR is constructed and mounted, we think that the misalignment of the SATR modules internally and versus the attached LCAL modules is about 100 μm.

The constants describing the misalignment of the four LCAL and SATR modules come from the general survey which was done in September 1989 and will be repeated in March 1990. The coordinates of the surveyed points were transformed to a set of three translational and three rotational constants which describe the misalignment of a rigid body completely. The reference point for the rotation (the one which is not modified by the rotation) is both for the LCAL and the SATR

$$\vec{x}_{ref} = \begin{pmatrix} 0 \\ 0 \\ \pm 262.5\, cm \end{pmatrix}$$

(262.5 cm is the z position of the Al front plate of the LCAL onto which the SATR is mounted.) The three translational constants $\delta_x, \delta_y, \delta_z$ give the three coordinates of the translation of the reference point as compared to the ideal position, whereas the rotational constants $\alpha_x, \alpha_y, \alpha_z$ give the rotation around the x', y', z' axis where the primed axes are parallel to the unprimed axes in the ideal ALEPH coordinate system but include the reference point $\vec{x}_{ref}$. Thus, the coordinates of a point measured in the local LCAL or SATR system (x', y', z') transform into ALEPH global coordinates (x, y, z) as follows:

$$\begin{pmatrix} x \\ y \\ z \end{pmatrix} = \begin{pmatrix} x' + \delta_x + \alpha_y(z' - z_{ref}) - \alpha_z y' \\ y' + \delta_y + \alpha_z x' - \alpha_x(z' - z_{ref}) \\ z' + \delta_z + \alpha_x y' - \alpha_y x' \end{pmatrix}$$

The misalignment constants are stored in the database banks LALI (for the LCAL) and SPOS (for the SATR). It should be noted that for the LCAL, all rotational constants are replaced by their negative values which is taken care of in all routines that use these constants.

In the GALEPH Monte Carlo program, the misalignment is taken care of by correcting the position of track elements which are transferred to the local LCAL resp. SATR coordinate system and then used to simulate hits in the subdetector. This happens in routines LCHIT which in turn calls LCFRAL to perform the calculations itself, resp. SAHIT.

In the JULIA reconstruction program, alignment correction is done in the routines LCORRC (for the LCAL) and SRALIG (for the SATR). In both cases, objects (clusters resp. tracks) are found assuming that the modules sit at the ideal place, and the alignment correction only modifies the parameters of the object.

Table 4 shows typical effects of the alignment corrections which were valid for the 1989 data. In order to compare local and global coordinates, points in the LCAL and SATR reference planes ($z = \pm 280\, cm$ resp. $z = \pm 254\, cm$) were selected and transformed to the global coordinate system. The points covered the full azimuthal range and a polar angle range of $50 \ldots 90\, mrad$ (approximately the combined LCAL and SATR acceptance) resp. $50 \ldots 150\, mrad$ (approximately the LCAL acceptance).

4.5 Dependence on Beam Parameters

The dependence of the luminosity measurement on beam parameters such as beam spot size, angle and position has been studied in detail for the workshops on polarization at

	$\vartheta = 50 \ldots 90\, mrad$	$\vartheta = 50 \ldots 150\, mrad$
$x - x'$	$-1.0 \ldots + 2.0\, mm$	$-1.2 \ldots + 2.2\, mm$
$y - y'$	$-2.5 \ldots - 1.3\, mm$	$-2.7 \ldots - 1.0\, mm$
$z - z'$	$-0.9 \ldots + 2.6\, mm$	$-1.8 \ldots + 3.2\, mm$

Table 4: LCAL and SATR alignment corrections for 1989 data

LEP [7]. We will see here that the uncertainty in the effective luminosity cross section from a realistic variation of beam parameters is completely negligible in the case of the standard asymmetric method five cuts. The details given here include simple, unrealistic cases of varying only one beam parameter at a time, keeping all other parameters at zero and are for illustration only.

The dependence of the lowest order Bhabha cross section on θ_{min} at the inner boundary is:

$$\frac{d\sigma}{\sigma} = \frac{2d\theta}{\theta}$$

The inner boundary of the LCAL is at about r=14 cm at z=280 cm or $\theta_{min} = 50 mrad$. A change of the inner radius of $700 \mu m$ translates into a change of cross section of 1%. We studied the loss of Bhabha events depending on beam parameters using the actual acceptance as simulated by our fast Monte Carlo. The results are shown in figure 6. They have been obtained using the same 10^6 events generated with the event generator OLDBAB for every case. The dotted line in figure 6 shows what we would have obtained using a symmetric acceptance. The dotted line in a) shows in fact about the slope that was expected from the simple formula given above. In reality, however, even using a symmetric acceptance, things are not as simple as suggested in a), where only a shift in x was simulated, keeping all other beam parameters exactly at zero. As demonstrated in [7], several effects tend to add quadratically. The largest effect comes usually from the bunch length. In figure 6 b) and c) we see the effect of the bunch length and the effective reduction in sensitivity to a shift in x if we consider the combined effect of a shift in x and a bunch length of 12.8 mm.

	$x_{shift} = 3mm$	$y_{shift} = 3mm$	$y_{tilt} = 1mrad$
symmetric cuts	3.7	1.0	-0.05
asymmetric cuts	-0.06	-0.003	-0.05

Table 5: loss of events in % depending on beam parameters, taking into account a constant bunch length of $\sigma_Z = 12.8mm$

The dependance is cancelled in first order using the asymmetric acceptance. The second order often has the opposite sign. Instead of a loss we get a very small gain in events when the beam is moved away from the origin. The result of a tilt is shown in f). A tilt of the beam does not change (in first order) the accepted cross section and the result of the

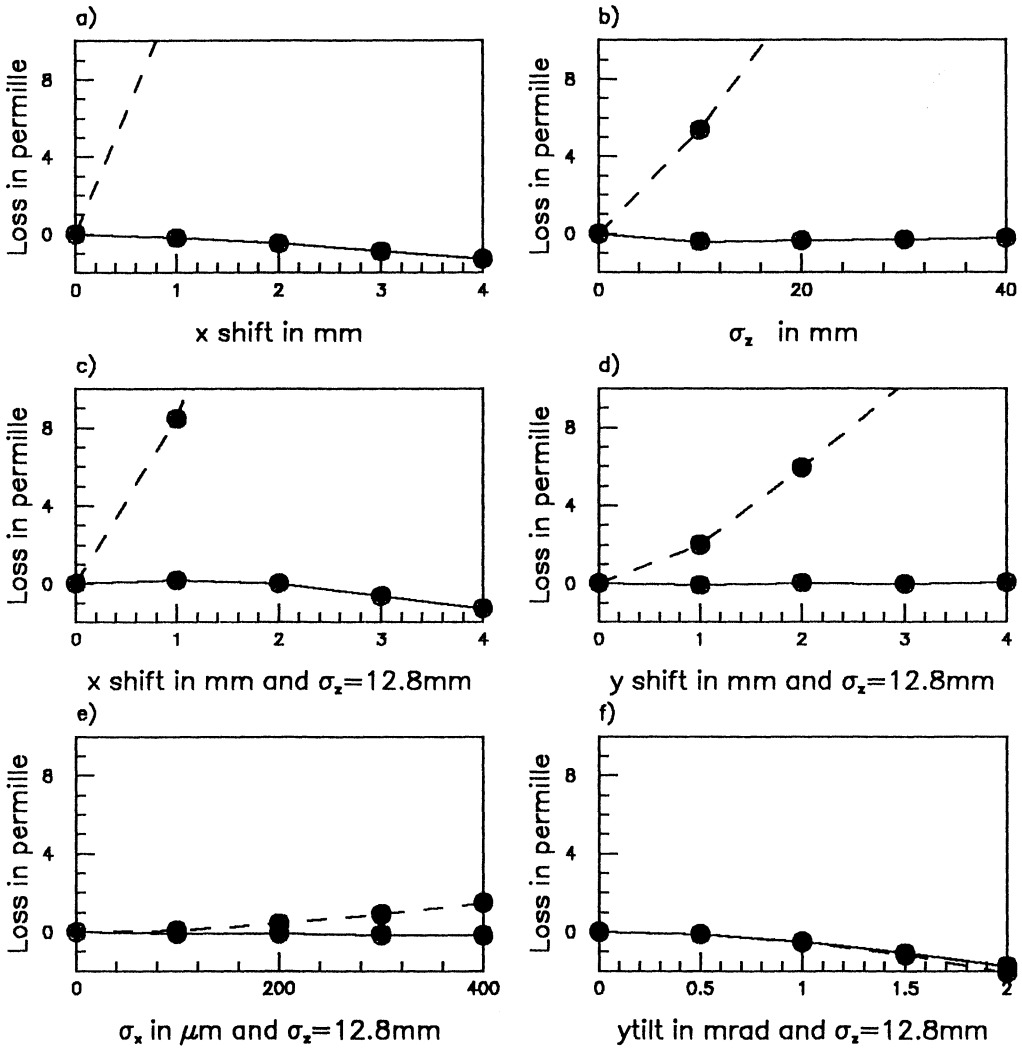

Figure 6: Loss of events in permille for changes of beam parameters. The solid line is for the standard selection with asymmetric cuts and the broken line for symmetric cuts.

symmetric and asymmetric case is therefore very small and similar. Some of the numbers that entered figure 6 are given in table 5.

5 Electroweak Interference

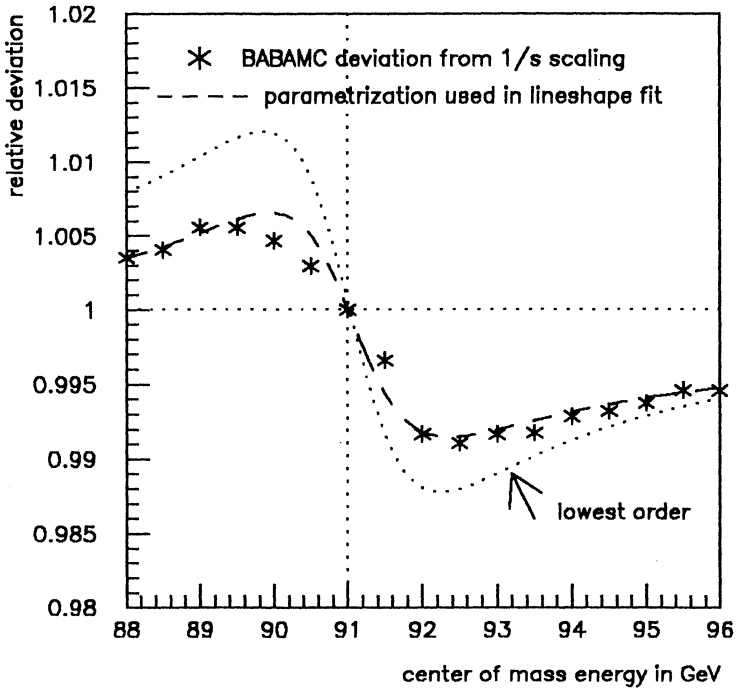

Figure 7: Electroweak correction in energy scaling

Bhabha scattering in the angular range considered here (about 50 - 110 mrad) is dominated by the t-channel. The interference with the Z-resonance is small. BABAMC is a complete electroweak $O(\alpha)$ program. The full GALEPH simulation using BABAMC has only been done on the peak assuming $\sqrt{s} = M_Z = 91.0 GeV$. The comparison to OLDBAB shows that the electroweak correction on the peak is not exactly zero but about $+0.3 \cdot 10^{-3}$. The extrapolation in the cross section to other energies follows the $1/s$ dependance of the cross section as in the pure QED case. The deviation from this is shown in Figure 7. It is parametrized following the suggestion of Hansen et al.:

$$\delta = \frac{1 + \frac{b(W-M_Z)+c}{(W-M_Z)^2+(\Gamma/2)^2}}{1 + \frac{c}{(\Gamma/2)^2}}$$

with $b = -0.018, c = 0.0028, M_Z = 91.0, \Gamma = 2.4, W = \sqrt{s}$.

The luminosity is first calculated using just the effective cross section scaled with $1/s$, since M_Z is not a priori known. The line shape fit uses than the parametrization to correct for the electroweak interference with the actual value of M_Z. The parametrization should be correct to about $1 - 2 \cdot 10^{-3}$.

6 Track reconstruction in the SATR

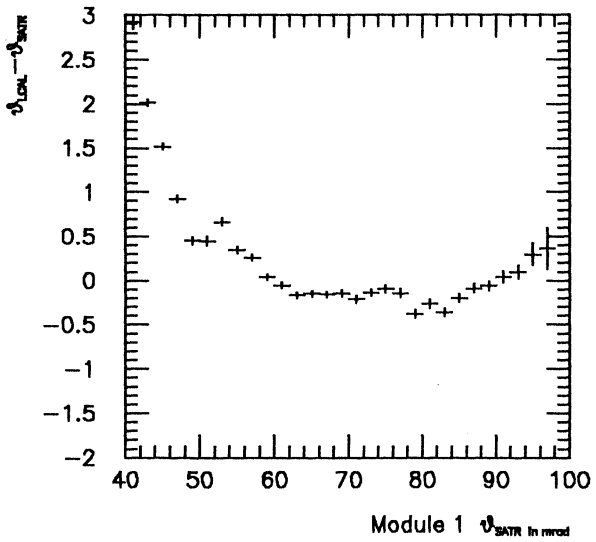

Figure 8: $\theta_{LCAL} - \theta_{SATR}$ as function of θ_{SATR}, for module 1 of the luminosity monitor. Data of 1989 running periods. Method 5. All units are mrad.

We illustrate the current state of the track reconstruction in the Small Angle TRacking device by comparing results with the LCAL measurements. In figure 8 the differences of the θ-measurements between LCAL and SATR are shown for module 1 as a function of θ as measured by the SATR. The data of the running periods 4001 to 5909 in 1989 have been used. The events are selected according to the so-called method 5. Figure 9 shows the distributions of the θ-differences for all 4 modules after a further cut in θ. The following conclusions may be drawn:

- The $\Delta\theta$ versus θ distributions show an upward bend at smaller θ. This bend is explained by shower leakage in the LCAL that results in too high θ values as measured by the LCAL at the lower edge of its acceptance.
- The width of the $\Delta\theta$ distributions is about 1 $mrad$ $(fwhm)$. This is larger than expected by about a factor of 1.5, as can be seen from the Monte Carlo simulation (fig. 10 and 11), and needs further investigation.
- All four modules show roughly the same behaviour. An exception is the shift of the $\Delta\theta$ distribution in module 3 for real data by about -0.5 mrad. Also this effect will be investigated.

There are good reasons to believe that the SATR results can still be improved. The current reprocessing of the data from 1989 with new calibration constants and a corrected treatment of the alignment shows already an improved track quality (the average number of hits used by a track fit increases by about 0.25, and more tracks are found). In addition, the following steps have been done to facilitate further improvements of the quality of the track reconstruction:

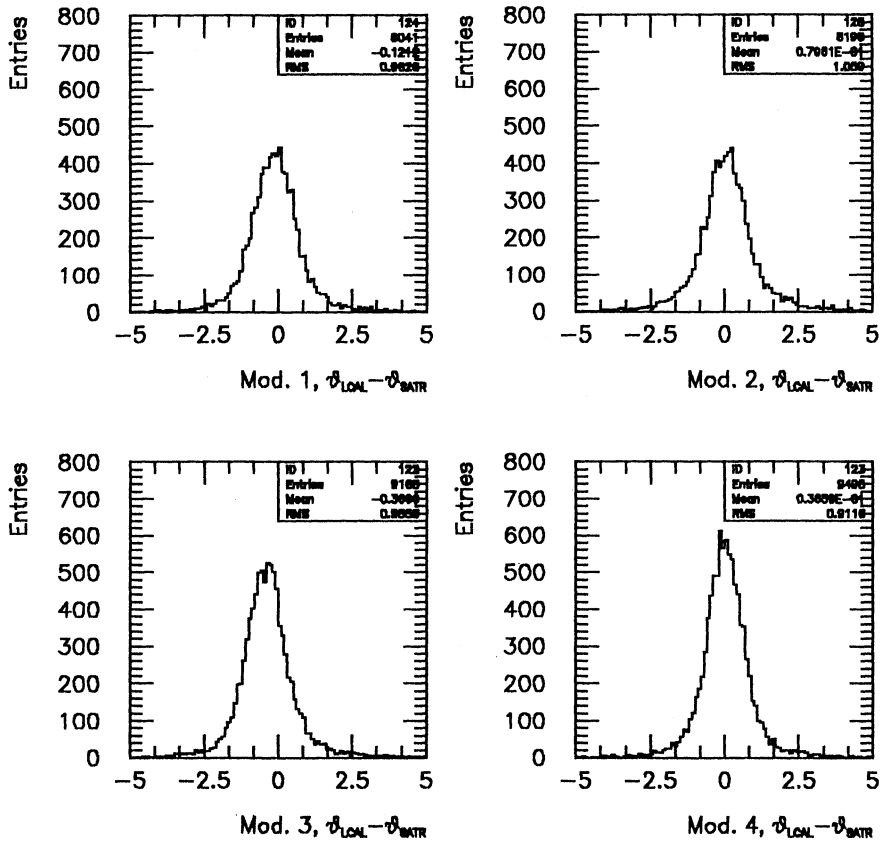

Figure 9: $\theta_{LCAL} - \theta_{SATR}$ in mrad for the 4 modules of the luminosity monitor. Data of 1989 running periods. Method 5. θ-range: 60 to 85 *mrad*.

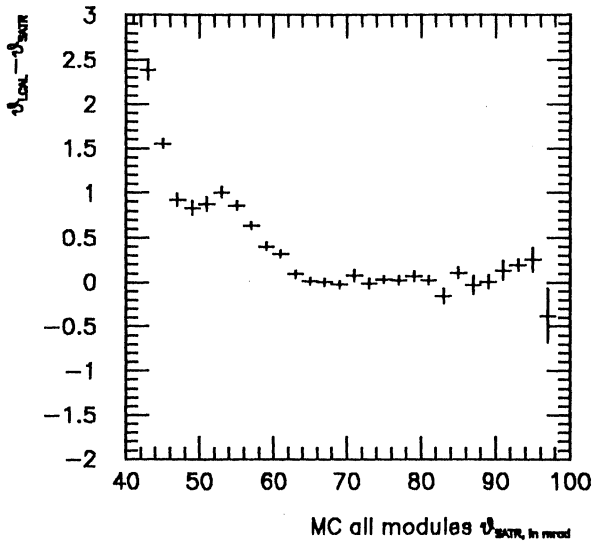

Figure 10: $\theta_{LCAL} - \theta_{SATR}$ as function of θ_{SATR}, using all 4 modules of the luminosity monitor. Data from full Monte Carlo simulation. Method 5. All angles are in mrad.

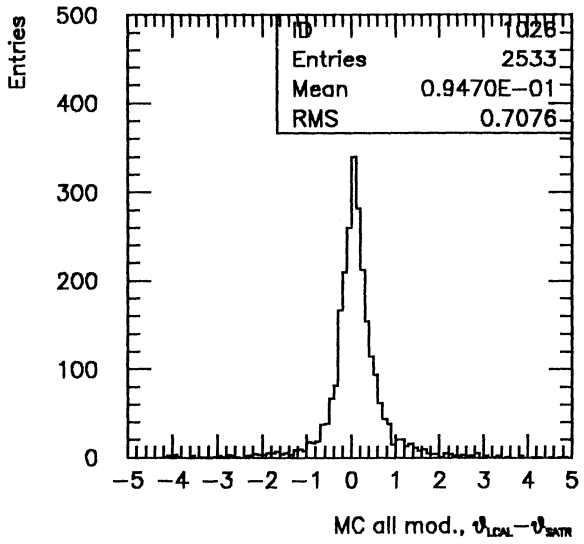

Figure 11: $\theta_{LCAL} - \theta_{SATR}$ in mrad using all 4 modules of the luminosity monitor. Data from full Monte Carlo simulation. Method 5. θ-range: 60 to 85 *mrad*.

- an automatic check of the raw data has been implemented;
- we have developed a special graphics program for the luminosity monitor;
- misalignment of the SATR can now be simulated in GALEPH;
- the track reconstruction can be repeated from the POT.

7 Summary,Conclusion

We have tried to give many details on work that has been done within the context of luminosity calculation. It has been shown that the method of calculating the luminosity by applying identical selection procedures to both data and Monte Carlo does not critically depend on small changes in the cuts. Our independent checks have led to some improvements in the code for the standard luminosity selection and in the calculation of the theoretical cross section. Given the small errors in the luminosity selection from the LCAL, we could not expect to get a significant reduction in uncertainties in using the SATR, but rather a confirmation and improved understanding. We verified indeed that the bias in the reconstructed position from LCAL showers near the edge is present as expected and correctly simulated in the Monte Carlo.

We tried to be complete in the discussion of small corrections and uncertainties from physics cross sections, radiative corrections and beam parameters using our fast Monte Carlo.

References

[1] ALEPH Collaboration, Determination of the Number of Light Neutrino Species,

Phys.Lett.B 231 (1989) 519

[2] F.Bird et al., Luminosity Errors, ALEPH NOTE 89-186

[3] ALEPH Collaboration, A precise determination of the Number of Families with Light Neutrinos and of the Z Boson Partial widths, CERN-EP/89-169, subm. to Phys.Lett.B

[4] F.A.Berends and R.Kleiss, Nucl.Phys. B228(1983) 537.

[5] F.A.Berends, W.Hollik and R.Kleiss, Nucl.Phys B304(1988) 712

[6] G.Altarelli et al. (ed.), Z Physics at LEP I, CERN 89-08

[7] G.Alexander et al. (ed.), Polarization at LEP, CERN 88-06, in particular Volume 2, Normalization in ALEPH, H.Burkhardt et al.

[8] H.Burkhardt, G.Bonvicini, Minutes and transparencies of the general Bhabha meeting held at CERN the 5-Feb-1990.

[9] H.Burkhardt, F.Jegerlehner, G.Penso, C.Verzegnassi Z.Phys. C43 (1989) 497
H.Burkhardt, Uncertainties from light quark loops, Proceedings of the Ringberg Workshop 3-7 April 1989, Ed. J.H.Kühn, Springer Verlag
H.Burkhardt, Light Quark Loops, Proceedings of the Nato Conference on Radiative Corrections, Brighton July 1989, to be published

[10] L3 Collaboration, Measurement of Z Decays to Hadrons, and a Precise Determination of Neutrino Species, L3 Preprint 4, December 24,1989

[11] F.Berends, R.Gastmans, Radiative Corrections in e^+e^- Collisions, in Electromagnetic Interactions of Hadrons, Vol.2, Donachie,Shaw (Eds), Pienum Publishing Corporation 1978
R.Kleiss, personal communication